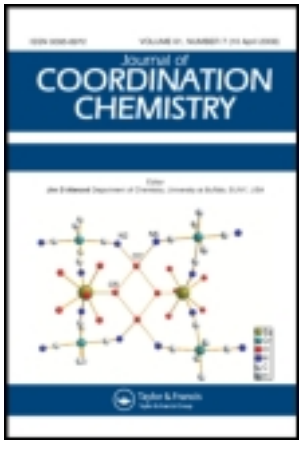

Journal of Coordination Chemistry
Publication details, including instructions for authors and subscription information:
http://www.tandfonline.com/loi/gcoo20

# Synthesis, spectroscopic, and biological activities of two binuclear complexes [Cu(II)(1-phenylamidino-O-methylurea)$_2$($H_2O$)]$_2$($Cl_2$)$_2$ and [Cu(II)(1-phenylamidino-O-i-butylurea)tmen]$_2$($Cl_2$)$_2$·2$H_2O$

S. Pramodini Devi [a], R.K. Bindiya Devi [a], M. Damayanti [b], N. Rajen Singh [a], R.K. Hemakumar Singh [a] & R.M. Kadam [c]

[a] Department of Chemistry, Manipur University, Imphal 795003, Manipur, India

[b] Department of Life Sciences, Manipur University, Imphal 795003, Manipur, India

[c] Radiochemistry Division, Bhabha Atomic Research Centre, Trombay, Mumbai 400085, Maharashtra, India

Published online: 29 Apr 2011.

To cite this article: S. Pramodini Devi, R.K. Bindiya Devi, M. Damayanti, N. Rajen Singh, R.K. Hemakumar Singh & R.M. Kadam (2011) Synthesis, spectroscopic, and biological activities of two binuclear complexes [Cu(II)(1-phenylamidino-O-methylurea)$_2$($H_2O$)]$_2$($Cl_2$)$_2$ and [Cu(II)(1-phenylamidino-O-i-butylurea)tmen]$_2$($Cl_2$)$_2$·2$H_2O$, Journal of Coordination Chemistry, 64:9, 1586-1601, DOI: 10.1080/00958972.2011.576341

To link to this article: http://dx.doi.org/10.1080/00958972.2011.576341

*Journal of Coordination Chemistry*
Vol. 64, No. 9, 10 May 2011, 1586–1601





# Synthesis, spectroscopic, and biological activities of two binuclear complexes [Cu(II)(1-phenylamidino-O-methylurea)$_2$($H_2O$)]$_2$($Cl_2$)$_2$ and [Cu(II)(1-phenylamidino-O-i-butylurea)tmen]$_2$($Cl_2$)$_2$·2$H_2O$

S. PRAMODINI DEVI†, R.K. BINDIYA DEVI†, M. DAMAYANTI‡, N. RAJEN SINGH†, R.K. HEMAKUMAR SINGH*† and R.M. KADAM§

†Department of Chemistry, Manipur University, Imphal 795003, Manipur, India
‡Department of Life Sciences, Manipur University, Imphal 795003, Manipur, India
§Radiochemistry Division, Bhabha Atomic Research Centre, Trombay, Mumbai 400085, Maharashtra, India

(*Received 19 August 2010; in final form 8 March 2011*)

EPR spectra of two copper(II) binuclear complexes, [Cu(II)(1-phenylamidino-O-methylurea)$_2$($H_2O$)]$_2$($Cl_2$)$_2$ (**1**) and [Cu(II)(1-phenylamidino-O-i-butylurea)tmen]$_2$($Cl_2$)$_2$·2$H_2O$ (**2**), at room temperature showed fine structure transitions ($\Delta M_s = \pm 1$) and a very weak half-field signal corresponding to forbidden transitions ($\Delta M_s = \pm 2$). The spectrum of **1** showed disappearance of normal and half-field transitions when cooled to 77 K, suggesting antiferromagnetical coupling dicopper complex which is also supported by the low magnetic moments ($\mu_{eff} = 1.64$ B.M.). The isotropic exchange interaction constant $J$ (41 cm$^{-1}$) for **2** indicated that interaction between the two spins of the binuclear complex is ferromagnetic, confirmed from the high magnetic moment value ($\mu_{eff} = 2.25$ B.M.). The binding of these complexes with calf thymus DNA suggested that these complexes interact with DNA by electrostatic or groove binding, not by intercalation. The two complexes have good antibacterial activity against tested bacteria responsible for urinary tract infection.

*Keywords*: Binuclear; EPR; DNA; Antimicrobial activity

## 1. Introduction

The interaction of transition metal complexes, particularly biocompatible copper(II) complexes, with DNA under physiological conditions has been a subject of extensive study [1–5]. In addition to biological relevance of transition metal complexes containing more than one metal, binuclear copper(II) complexes have been used extensively to derive magneto structural correlations to understand spin–spin coupling in different structures [6]. Magnetic parameters measured by EPR are related to the structure of paramagnetic species, the number of ligands, the bonding parameters, and arrangement of ligands around the metal [7]. In most cases, where site symmetry at the paramagnetic

*Corresponding author. Email: rkhemakumar@rediffmail.com


ISSN 0095-8972 print/ISSN 1029-0389 online 
DOI: 10.1080/00958972.2011.576341

ions is identical and exchange interaction is mediated through a shared ligand, formation of antiferromagnetically coupled dimers result in localized $S = 0$ singlet state. Ferromagnetic interaction can arise from the interaction of unpaired spins at different site symmetries in bimetallic systems and offers a greater variety of magnetic order at low temperatures [8]. Therefore, systems containing two strongly coupled unpaired electrons (with effective spin $S = 1$) attract considerable attention because of their interest to inorganic and bioinorganic chemists [9].

Many papers have been published on supramolecular architectures based on $[CuL_2]^{2+}$ cations in which copper(II) is coordinated by tetradentate *bis*(amidino-O-alkylurea) ligands which have hydrogen bonding potential (eight N–H donor centers and two oxygen acceptor centers). Transition metal complexes containing ligands with hydrogen bonding capabilities have been used to bind DNA bases and other anions and to construct networks of coordinated complexes connected through intermolecular interactions [10]. DNA provides a range of binding sites and binding modes for covalent and non-covalent interactions, including intercalation, groove bindings, electrostatic force and hydrogen bonds with metal complexes. Interest in metal complex binding to DNA has been motivated by the desire to understand the basics of these interactions and also to develop metal complexes into anti-inflammatory, antifungal, antibacterial, or anticancer reagents [11]. We have investigated antibacterial and antifungal properties of *bis*(1-*n*-butylamidino-O-alkylurea)copper(II) complexes [7]. Recently, Chaveerach *et al*. [12] investigated DNA binding and cleavage of copper(II) complexes with 1-amidino-O-methylurea and N-methylphenyl-amidino-O-methylurea and their antibacterial activities. DNA binding interactions on *bis*(1-amidino-O-alkoxyethylurea)nickel(II)nitrate complexes have also been reported [13].

In continuation of our effort to synthesize binuclear copper(II) complexes containing ligands with versatile hydrogen bonding capabilities [7, 14–17], we report here spectroscopic investigations on two binuclear complexes, antiferromagnetically coupled $[Cu(II)(1\text{-phenylamidino-O-methylurea})_2(H_2O)]_2(Cl_2)_2$ and ferromagnetically coupled $[Cu(II)(1\text{-phenylamidino-O-i-butylurea})tmen]_2(Cl_2)_2 \cdot 2H_2O$, for insight into the chemical and structural factors that govern the formation of binuclear complexes. The interaction with calf thymus (CT) DNA was investigated by electronic absorption titration, quenching the fluorescence of the DNA-ethidium bromide (EB) system, and DNA thermal denaturation studies. The antibacterial activity of the two complexes is also reported.



## 2. Experimental

### 2.1. *Methods and materials*

All chemicals were of reagent grade. Phenyldicyanodiamide (PD) was prepared by following published procedure [18]. The purity was checked by IR spectra.

### 2.2. *Preparation of complexes*

**2.2.1. $[Cu(II)(1\text{-phenylamidino-O-methylurea})_2(H_2O)]_2(Cl_2)_2$ (1).** This complex was prepared according to published procedure [19] by refluxing PD (2 mol) and cupric

chloride dihydrate (1 mol) in methanol on a water bath for 5 h. Color – light violet, Yield – 75%, m.p.: 148°C, $\lambda_{max}$ (DMF) – 18382 $cm^{-1}$ ($\varepsilon = 108\,(mol\,L^{-1})^{-1}cm^{-1}$), $\mu_{eff}$ – 1.64 B.M., Anal. Calcd for $C_{36}H_{52}Cl_4Cu_2N_{16}O_6$: C, 40.26; H, 4.84; N, 20.87; and Cu, 11.83. Found: C, 40.42; H, 4.75; N, 21.10; and Cu, 11.80.

**2.2.2. [Cu(II)(1-phenylamidino-O-i-butylurea)tmen]$_2$(Cl$_2$)$_2 \cdot 2H_2O$ (2).** This mixed ligand complex was prepared by the following two steps:

1. Preparation of dichloro-mono-(1-phenylamidino-O-i-butylurea)copper(II): The complex was prepared using our published procedure [15] by refluxing cupric chloride (1 mol) and PD (1 mol) in *iso*-butanol on a steam bath for 2 h. The intense blue complex was filtered off immediately, washed several times with acetone, and dried in air. Color – intense blue, Yield – 80%, m.p.: 195°C, Anal. Calcd for $C_{12}H_{18}Cl_2CuN_4O$: C, 39.07; H, 4.88; N, 15.19; and Cu, 17.23. Found: C, 38.92; H, 4.81; N, 15.20; and Cu, 17.31.
2. Preparation of [Cu(II)(1-phenylamidino-O-i-butylurea)tmen]$_2$(Cl$_2$)$_2 \cdot 2H_2O$ (**2**), where tmen = N,N,N′,N′-tetramethylethylenediamine: The blue dichloromono-(1-phenylamidino-O-i-butylurea)copper(II) (0.1 mol) was dissolved in hot ethanol and 0.1 mol of tmen was added with constant stirring in a beaker on a steam bath for 30 min. After keeping overnight in a refrigerator, the complex was obtained, washed repeatedly with ethanol, and dried in air. Color – violet, Yield – 65%, m.p.: 128°C, $\lambda_{max}$(DMF) – 19880 $cm^{-1}$ ($\varepsilon = 100\,(mol\,L^{-1})^{-1}cm^{-1}$), $\mu_{eff}$ – 2.25 B.M., Anal. Calcd for $C_{36}H_{72}Cl_4Cu_2N_{12}O_4$: C, 42.98; H, 7.16; N, 16.71; and Cu, 12.63. Found: C, 42.99; H, 7.04; N, 16.75; and Cu, 12.58.

### 2.3. *Physical measurements*

Microanalyses were performed on a C, H, N analyzer Perkin Elmer 2400 model; IR spectra were recorded as KBr disks on a Shimadzu FTIR-8400S. The amount of copper was determined by fusing the complex with $KHSO_4$, then extracting with a mixture of $HNO_3$ and $H_2SO_4$ and finally by performing an iodometric titration. Electronic spectra were recorded on a Perkin Elmer UV-Vis Lamda 35 spectrophotometer. EPR experiments were conducted using a BRUKER ESP-300 spectrometer operated at X-band frequency (9–10 GHz) with 100 kHz field modulation. DPPH was used as field marker. Temperature was varied in the range 77–400 K using variable temperature accessory Eurotherm BVT 2000 with liquid nitrogen as coolant in a flow system. The EPR parameters for copper complexes have been precisely determined from the calculated spectra, which were obtained with Bruker SIMFONIA program based on perturbation theory (Weber, R.T., WIN-EPR SIMFONIA manual, 1995). Magnetic moments at room temperature ($\mu_{eff}$) were measured using Sherwood scientific susceptibility balance (MSB). Molar conductance in MeOH was measured at room temperature on an Eutech instrument con 510 conductivity. Thermal studies of the compounds were carried out in air with a Shimadzu thermal analyzer DT-30. The fluorescence spectra were recorded by a Perkin Elmer LS55 spectrophotometer.

### 2.4. *DNA interaction studies*

CT-DNA and Tris–HCl molecular biological grade were purchased from Merck (India), EB was obtained from Sigma and all other chemicals were of spectroscopic grade. DNA concentration was determined by absorption spectroscopy using the molar absorption coefficient ($6600\,(\mathrm{mol\,L^{-1}})^{-1}\mathrm{cm}^{-1}$) at 260 nm [20]. Solution of CT-DNA in $5\,\mathrm{mmol\,L^{-1}}$ Tris–HCl/$50\,\mathrm{mmol\,L^{-1}}$ NaCl (pH = 7.4) buffer gave ratio of UV absorbance at 260 and 280 nm, $A_{260}/A_{280}$ ~1.9 indicating that the DNA was sufficiently free of protein [21]. The stock solution of DNA prepared in the buffer kept at 4°C was used within 4 days. Tris–HCl buffer solution was prepared using deionized, sonicated triply distilled water.

DNA absorption experiments were carried out by varying the DNA concentration and maintaining the complex concentration constant. Absorbance values were recorded after each successive addition of DNA solution. The intrinsic binding constant ($K_b$) was determined according to the following equation [22]

$$[\mathrm{DNA}]/(\epsilon_A - \epsilon_F) = [\mathrm{DNA}]/(\epsilon_B - \epsilon_F) + 1/K_b(\epsilon_B - \epsilon_F)$$

where $\epsilon_A$, $\epsilon_F$, and $\epsilon_B$ correspond to apparent, free, and bound metal complexes extinction coefficients, respectively. In the plot $[\mathrm{DNA}]/(\epsilon_A - \epsilon_F)$ *versus* [DNA], $K_b$ is given by the ratio of the slope to intercept.

The fluorescence spectral method using EB as reference was used to determine the relative binding properties of the complexes to CT-DNA. Fluorescence intensities of EB at 597 nm with an excitation wavelength of 274 nm were measured at different complex concentrations. The apparent binding constant ($K_{app}$) was calculated using the following equation [23]:

$$K_{EB}\,[\mathrm{EB}] = K_{app}[\mathrm{complex}]$$

where the complex concentration was the value at a 50% reduction of the fluorescence intensity of EB and $K_{EB} = 1.0 \times 10^7\,(\mathrm{mol\,L^{-1}})^{-1}$, $[\mathrm{EB}] = 1.3\,\mu\mathrm{mol\,L^{-1}}$.

DNA melting experiments were carried out by monitoring the absorption intensity of CT-DNA (260 nm) at various temperatures both in the absence and presence of the complexes. Measurements were carried out using a Perkin Elmer Lambda 35 spectrophotometer equipped with a Peltier temperature controlling programmer (PTP6). The experiments were repeated at least three times to get the average value of the melting temperature.

### 2.5. *Antimicrobial activity*

The antimicrobial activity was performed by filter paper disc diffusion technique [24]. The blood agar was used to culture the bacteria. The molten blood agar medium (45°C) was poured into sterile glass petri plates and allowed to solidify. Overnight broth cultures of bacteria ($10^6\,\mathrm{cfu\,mL^{-1}}$) were swabbed on the solidified media. The sterile filter paper discs were loaded with different concentrations of synthesized complexes and standard antibiotic, namely gentamycin sulfate, on separate discs by dipping the discs in respective solutions for 5 s. Discs with DMSO served as a control. Then, these discs were gently lifted and kept on the inoculated plates. The plates were then maintained at room temperature for 2 h to allow diffusion of the solutions into the

medium and incubated at $37 \pm 2^{\circ}C$. Inhibition was recorded by measuring the diameter of the inhibition zone at 24 h. The experiment was repeated three times with three replicates of each treatment. The antimicrobial activities of the synthesized complexes were compared with the standard antibiotic, namely gentamycin sulfate.

## 3. Results and discussion

### 3.1. *Electronic spectra*

The unusual violet coloration of **1** and **2** arises from the strong ligand field in $[CuN_4]^{2-}$. The electronic spectra of solid complexes showed a broad band at *ca* 20,000 $cm^{-1}$ due to high-energy d–d electronic transitions. This absorption is similar to that observed in square planar copper(II)-O-alkyl-1-amidinourea complexes [25]. Absorption spectra of **1** and **2** recorded in DMF showed typical broad absorption bands at *ca* 18,382 $cm^{-1}$ for **1** and 19,880 $cm^{-1}$ for **2** which may be due to axial ligation of solvent. An intense absorption at *ca* 25,900 $cm^{-1}$ in the solution spectra is due to charge transfer [25].

### 3.2. *IR spectra*

IR spectrum of PD (figure S1) shows $\nu_{C\equiv N}$ at 2167 $cm^{-1}$ and $\nu_{C=N}$ at 1656 $cm^{-1}$ [14, 15, 26]. In IR spectra of the complexes (figures S2 and S3), there is no band at 2167 $cm^{-1}$, suggesting the absence of a nitrile group in these complexes. Instead the complexes have a very strong $\nu_{a(C-O-C)}$ stretch at *ca* 1190 $cm^{-1}$ and $\nu_{s(C-O-C)}$ at *ca* 962 $cm^{-1}$ [27]. The lowering of $\nu_{C=N}$ to 1571–1573 $cm^{-1}$ and appearance of $\nu_{C-N}$ at 1392 $cm^{-1}$ indicates coordination through C=N of phenylamidine. The fragment N=C−O−C of 1-phenylamidino-O-alkylurea is delocalized and the bond order of the =C−O− group is raised, giving a new $\nu_{C=N}$ at 1683–1689 $cm^{-1}$ after coordination [14, 15, 27–29]. The IR spectrum of **1** shows weak bands at 860 and 898 $cm^{-1}$ for $\rho_r$ and at 560 $cm^{-1}$ for $\rho_{wagg}$ of coordinated water [30] and at 440 $cm^{-1}$ for Cu–O bonding [31]. In the IR spectrum of **2**, a broad and strong bands at 3261 $cm^{-1}$ is assigned to $\nu_{N-H}$ of the primary amine [32, 33] and medium bands at 3639 and 1640 $cm^{-1}$ may be assigned to $\nu_{(O-H)}$ and $\nu_{(H-O-H)}$, respectively, for lattice water present in the complex [34, 35]. A band at 1092 $cm^{-1}$ is due to $\nu_{C-C}$ of N,N,N′,N′ tetramethylethylenediamine [36]. In the IR spectrum of **2** recorded carefully after heating the complex and KBr at 100°C, a decrease in band intensity assigned for $\nu_{(OH)}$ was observed, suggesting loss of water in this temperature range which is supported by thermal studies of the complex.

### 3.3. *Thermal studies*

Thermal analysis data of **1** showed 19% weight loss in the range 150–240°C, which may be due to the combined loss of two coordinated waters along with ligands. In the thermal analysis data of **2**, loss of water started at *ca* 50°C and was completed at *ca* 100°C, indicating the loss of lattice water. Successive changes of the complex may be suggested due to the loss of ligands. The weight loss at 550°C is accompanied by an exotherm which may be due to oxidation during heating.

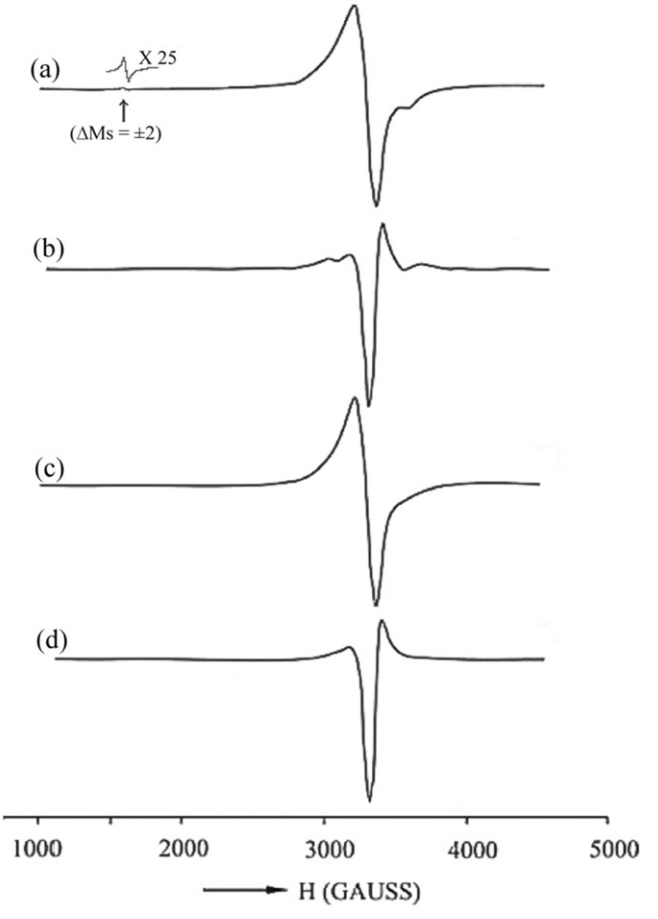


Figure 1. EPR spectra of **1** in the solid state: (a) at 300 K; (b) second derivative spectrum at 300 K; (c) at 77 K; and (d) second derivative spectrum at 77 K.

### 3.4. *EPR spectra*

The EPR spectrum of **1** at room temperature showed an intense resonance at $g = 2.050$ superimposed on a very weak doublet ($\Delta M_s = \pm 1$). In addition to this, a very weak half-field signal at *ca* 1630 G due to $\Delta M_s = \pm 2$ transition was seen (figure 1a); the simulated spectrum is shown in figure 1b. An important observation in the EPR spectrum of this complex was the disappearance of normal and half-field transitions $\Delta M_s = \pm 1$ and $\Delta M_s = \pm 2$, respectively, of binuclear complex when cooled to 77 K (figure 1c). The decrease in the intensity of allowed and forbidden transitions suggests antiferromagnetic coupling between two interacting Cu(II) ions [37]. The low $\mu_{eff}$ (1.64 B.M.) value at room temperature further supports this observation.

EPR spectrum of **2** (figure 2a) recorded in the solid state consists of two intense bands separated by 500 G with some perpendicular components. On either side of these intense bands, a signal consisting of several narrow lines nearly double the perpendicular separation was observed. The EPR studies conclusively establish the formation of

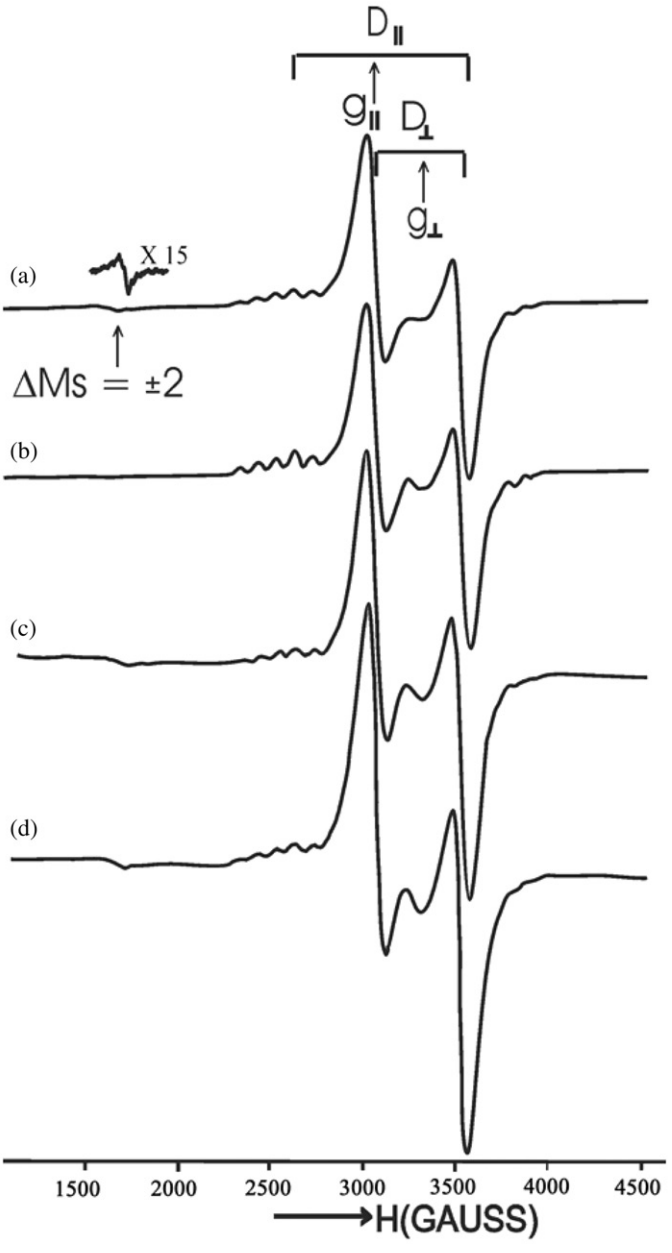


Figure 2. EPR spectra of **2** in the solid state: (a) at 300 K, (b) simulated spectrum using the EPR parameters as given in table 1; (c) at 140 K; and (d) at 94 K.

binuclear species in [Cu(II)(1-phenylamidino-O-i-butylurea)tmen]$_2$(Cl$_2$)$_2 \cdot 2$H$_2$O (**2**) (presence of a weak half-field signal at magnetic field *ca* 1600 G due to $\Delta M_s = \pm 2$ transition which is forbidden and therefore weak and an intense doublet centered at *ca* 3325 G having zero field splitting, $D = 0.0485\,\text{cm}^{-1}$ due to allowed transition $\Delta M_s = \pm 1$).

The high magnetic moment 2.5 B.M. also supports the formation of a binuclear complex. EPR spectra of **1** in MeOH (figure S4) and **2** in DMF (figure S5) at low temperature consist of mononuclear species indicating dissociation of weak hydrogen bonds responsible for stacking of two mononuclear species in the solid state, which is also supported by conductance in MeOH ($\Lambda_M = 154$–$168\,\Omega^{-1}cm^2mol^{-1}$ for bi-univalent electrolyte). The two unpaired electrons are delocalized on two coppers ($^{63}$Cu, $I = 3/2$, abundance 69.2%; $^{65}$Cu, $I = 3/2$, abundance 30.8%) resulting in a seven-line hyperfine structure with intensity following binomial distribution which is clearly seen in the low-field parallel component. The resulting hyperfine coupling constant in **1** and **2** are reduced to half ($A = 95$ G) compared to hyperfine coupling constant of the corresponding mononuclear complexes ($A = 210$ G) in frozen DMF or MeOH. In **2,** a mixture of mononuclear and binuclear species forms (figure S5). Assuming that the two monomer planes of **2** are parallel in a dimer, and the principal axes of the $g$ and $A$ tensors coincide, various spin interactions in the dimer system are described to a good approximation by the spin Hamiltonian (1)

$$H = H.g.S + H_d + S.A.I + JS_1.S_2 \tag{1}$$

where $S = S_1 + S_2$, $I = I_1 + I_2$ and $g$ and $A$ are the $g$ tensor and the hyperfine tensor, D and E the second-order crystal field terms with axial and rhombic structure parameters, and $S$ the total spin of the electron, appropriate for the monomer [38]. In polycrystalline sample, EPR signals have been simulated by generating 9000 random orientations of the magnetic field and by summing the corresponding 9000 absorptions. The final signal was obtained by performing a convolution (Gaussian or Lorentzian line shape) of each transition line, adding all contributions and calculating the first-derivative signal; the line width of each component has been optimized to obtain the best accord with observed experimental values. Errors in calculating the spin Hamiltonian parameters $g$, $A$ (hyperfine coupling constant) and D (zero field splitting) are $\pm 0.0002$, $\pm 2.0$ and $\pm 5.0$ G, respectively. There is a close resemblance between the experimental (figure 2a) and simulated spectra (figure 2b) suggesting overall goodness-of-fit. The EPR parameters $g_{||}$, $g_{\perp}$, and $A_{||}^{Cu}$ were measured from anisotropic spectra of magnetically dilute copper complexes in frozen solution and are shown in table 1 along with EPR parameters of copper(II) mononuclear (M) and binuclear (B) complexes with different ligands for comparison. When the $g$ tensor is axially symmetric and $g_{||}$ axis is parallel to the vector joining the copper(II) ions, $H_d$ can be rewritten [39] in the form (2) where $D = (3/4)\ g_{||}^2\beta^2\langle(1-3\cos^2\theta)/r^3\rangle_{max}$ and $\theta$ is the angle between $g_{||}$ and magnetic field direction

$$H_d = D[S_z^2 - (1/3)S(S+1)] \tag{2}$$

The spin Hamiltonian parameters for **2** are typical of those values for copper(II) complexes coordinated to nitrogen ligands with a square planar coordination. We have evaluated the angle $\xi$ (33°) using the equation $g_z^2 = g_{||}^2\cos^2\xi + g_{\perp}^2\sin^2\xi$ [38], where $g_{||}$ (2.1943) and $g_{\perp}$ (2.0530) represent $g$ values for the mononuclear complex, $\xi$ is the angle between Cu–Cu direction, and the $g_{||}$ is replaced by $g_z^2$ (2.1521) as $g_{||}$ and Cu–Cu direction for binuclear complex (**2**) do not coincide. The isotropic exchange interaction constant $J$ or the separation between the singlet and triplet was calculated from the temperature dependence of the intensity of half-field signal ($\Delta M_s = \pm 2$) [40]. The increase in intensity of the EPR signal with lowering of temperature is much more than

Table 1. EPR parameters of copper(II) mononuclear (M) and binuclear (B) complexes with different ligands.

| Matrix | $g_{\|\|}$ | $g_{\perp}$ | $g_{iso}$ | $A_{\|\|}$ (G) | $A_{\perp}$ (G) | $A_{iso}$ (G) | $D$ ($cm^{-1}$) | $J$ ($cm^{-1}$) | $R$ (A°) | References |
|---|---|---|---|---|---|---|---|---|---|---|
| [Cu(1-PhAB$^{i}$UH)$Cl_2$] (M) | 2.2075 | 2.0450 | 2.0992 | | | | | | | [15] |
| [Cu(II)(1-PhAMUH)tn]$Cl_2$ (M) | 2.1774 | 2.0400 | 2.0858 | 210 | 30 | 90 | | | | [15] |
| [Cu(1-AMUH)$_2$]$Cl_2$ (M) | 2.24 (RT) | 2.06 (RT) | 2.1200 | 218 | 25 | 89 | | | | [19] |
| | 2.176 (77 K) | 2.058 (77 K) | 2.0973 | | | | | | | |
| [Cu(II)1-PhAB$^{i}$UH)en]$_2$($H_2O$)$_2$($Cl$)$_2$ (B) | 2.1640 | 2.0525 | 2.0897 | 100 | | | 0.0493 (300 K) | +55 | 3.99 | [15] |
| | 2.1650 | 2.0425 | 2.0833 | | | | 0.0530 (77 K) | | | |
| [Cu(II)1-PhAB$^{i}$UH)tn]$_2$($H_2O$)$_2$($Cl$)$_2$ (B) | 2.1730 | 2.0485 | 2.0900 | 100 | | | 0.0505 | +50 | 3.98 | [15] |
| | | | | | | | 0.0525 (77 K) | | | |
| [Cu(1-PhABUH)en($H_2O$)]$Cl_2$ (B) | 2.1200 | 2.0525 | 2.0750 | 90 | | | 0.0525 | +57 | 4.00 | [14] |
| [Cu(1-PhAMUH)$SO_4$]$_2$ (B) | 2.2383 | 2.1773 | 2.1976 | | | | 0.0225 | +27 | 4.70 | [14] |
| ($Cu^{2+}$)$_2$in(dl)-(tart)$_2^{4-}$ (B) | 2.224 | 2.0860 | 2.1320 | 82 | | | 0.0057 | −18 | 3.85 | [37] |
| ($Cu^{2+}$)$_2$in$CeO_2$ (B) | 2.2079 | 2.0403 | 2.0962 | 85 | 13.5 | 37.5 | 0.066 | −52 | 4.50 | [38] |
| Complex **1** (B) | | ~2.050 | | | | | 0.0600 | | | |
| Complex **2** (B) | 2.1521 | 2.0303 | 2.0709 | 100 | | | 0.046 | +41 | 3.92 | |

PhAB$^{n}$UH = phenylamidino-O-*n*-butylurea; PhAMUH = phenylamidino-O-methylurea; PhAB$^{i}$UH = phenyamidino-O-i-butylurea; AMUH = amidino-O-methylurea; en = 1,2-diaminoethane; tn = 1,3-diaminopropane.
Error in $g$ is ±0.0001 and in $A$ is ±2.8 MHz.

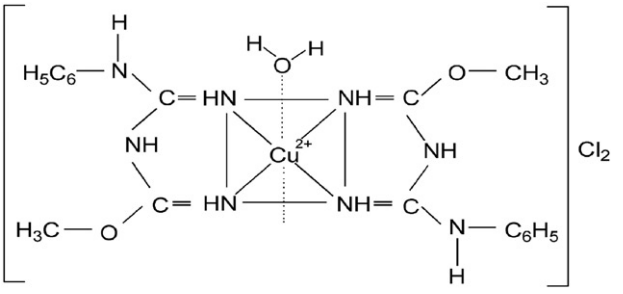


Figure 3. Proposed structure of [Cu(II)(1-phenylamidino-O-methylurea)$_2$($H_2O$)]$Cl_2$.

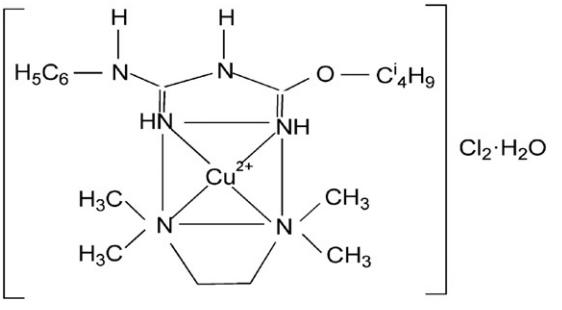


Figure 4. Proposed structure of [(Cu(II)(1-phenylamidino-O-i-butylurea)tmen]$Cl_2 \cdot H_2O$.

expected from the Boltzmann population difference within the triplet manifold. It appears that the isotropic exchange interaction between interacting spins of the binuclear complex is ferromagnetic. The $J$ value estimated for **2** was 41 $cm^{-1}$. The average distance $r$ between the two unpaired electrons was calculated using $D = 3g^2ß^2/2r^3 = 1.39 \times 10^4$ $(g/r^3)$ [41] and $r$ for **2** is given in table 1, where $D$ is in gauss and $r$ in Angstroms. The plausible structure of **1** may consist of two discrete monomers $[Cu(1\text{-phenylamidino-O-methylurea})_2]^{2+}$ with two coordinated waters. Cu(1-amidino-O-methylurea)$_2$ is nearly planar, with Cu located in centrosymmetric square planar coordination of four equivalent N=H donors. The discrete Cu(1-amidino-O-methylurea)$_2$ molecules form parallel planes. Water is coordinated to copper, however, the distance between Cu and apical water is large. The perfect square planar coordination of four equivalent nitrogen donors around Cu(II) is further confirmed by recording the EPR spectrum of **1** in MeOH where the perpendicular component clearly shows well resolved nine components of superhyperfine structure with superhyperfine coupling constant of the order of 15 G typical of nitrogen coordination ($^{14}N$, $I = 1$, 100% abundance). In complex **2**, there is unresolved superhyperfine structure seen on the perpendicular component as Cu is coordinated to two types of nitrogen donors. On the basis of our experimental evidence, we suggest the most probable structures of the monomers in figures 3 and 4 for **1** and **2**, respectively.

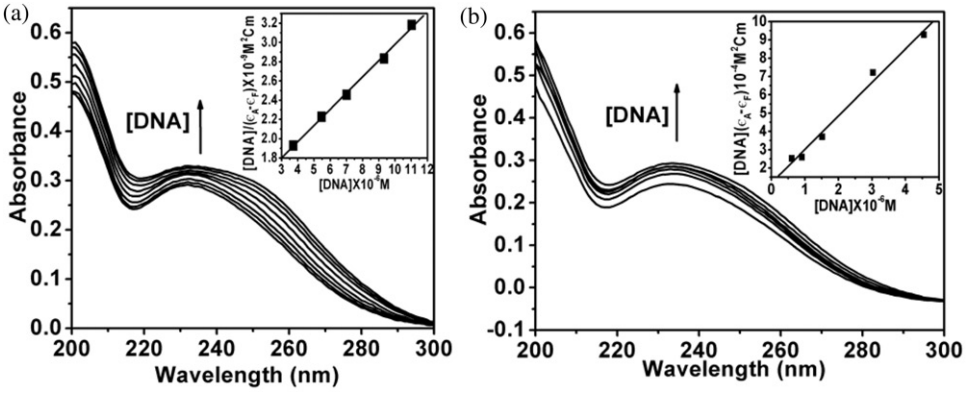


Figure 5. Absorption titration spectra of complexes in the absence (bottom curve) and presence (subsequent curves) of CT-DNA from 0 to 15 μmol $L^{-1}$. [complex] = 10 μmol $L^{-1}$. Arrow shows the absorbance change with increasing DNA concentrations and inset plot of [DNA]/($\epsilon_A - \epsilon_F$) *vs.* [DNA] with **1**, (a) and **2**, (b).

### 3.5. *DNA interaction studies*

Absorption titration was carried out to investigate the binding affinity of the complexes with CT-DNA. Intercalation into the DNA helix generally results in hypochromism and bathochromism of the absorption, due to strong stacking intercalation between the aromatic chromophore and DNA base pairs [42–44]. Absorption intensity of a complex is increased (hyperchromism) upon increasing the concentration of CT-DNA due to degradation of the DNA helix structure [45]. The extent of hyperchromism is indicative of the amount of intercalation. The absorption spectra of [Cu(II)(1-phenylamidino-O-methylurea)$_2$($H_2O$)]$_2$($Cl_2$)$_2$ and [Cu(II)(1-phenylamidino-O-i-butylurea)tmen]$_2$($Cl_2$)$_2$ · 2$H_2O$ (figure 5) in the presence of increasing CT-DNA concentration show that as the concentration of DNA increases the band at 232 nm exhibits hyperchromism, indicating partial or non-intercalative interactions between the complexes and DNA. The values of $K_b$ for **1** and **2** are $0.13 \times 10^6$ and $1.5 \times 10^6$ $(\text{mol L}^{-1})^{-1}$, respectively.

EB emits intense fluorescence in the presence of DNA, due to strong intercalation between adjacent DNA base pairs. The addition of a second DNA binding molecule can quench the DNA-EB adduct emission by either replacing the EB or by accepting the excited state electron of EB through a photoelectron transfer mechanism [46, 47]. The emission spectra of EB bound to DNA with various concentrations of **1** and **2** (figure 6) reduce in intensity, indicating that the complex binds to DNA. The association constant ($K_{app} \times 10^{-6}$ $(\text{mol L}^{-1})^{-1}$) values of **1** and **2** are 2.0 and 2.2, respectively.

Thermal behavior of DNA in the presence of metal complex can give insight into their conformational changes when temperature increases and information about the interaction strength of the complex with DNA. Double-stranded DNA tends to gradually dissociate to single strands with increase in solution temperature and generates a hyperchromic effect on the absorption spectra of DNA bases ($\lambda_{max} = 260$ nm). In order to identify this transition process, the melting temperature ($T_m$), which is defined as the temperature where half of the total base pairs are

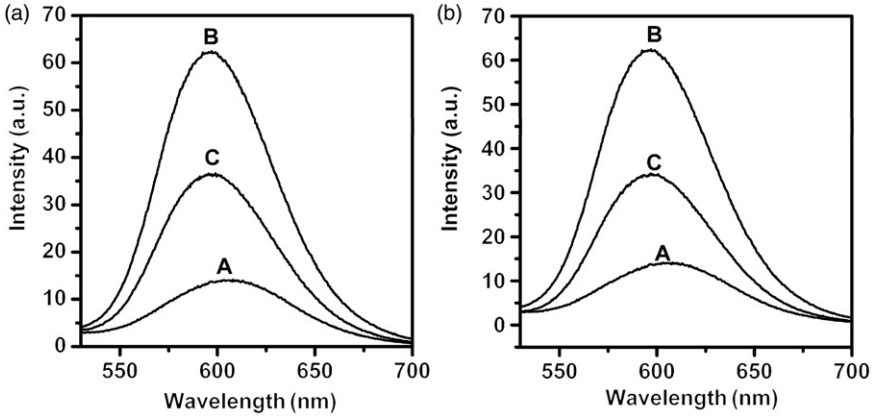


Figure 6. Emission spectra of EB in the (A) absence, (B) presence of DNA and (C) DNA-EB with **1**, (a) and **2**, (b).

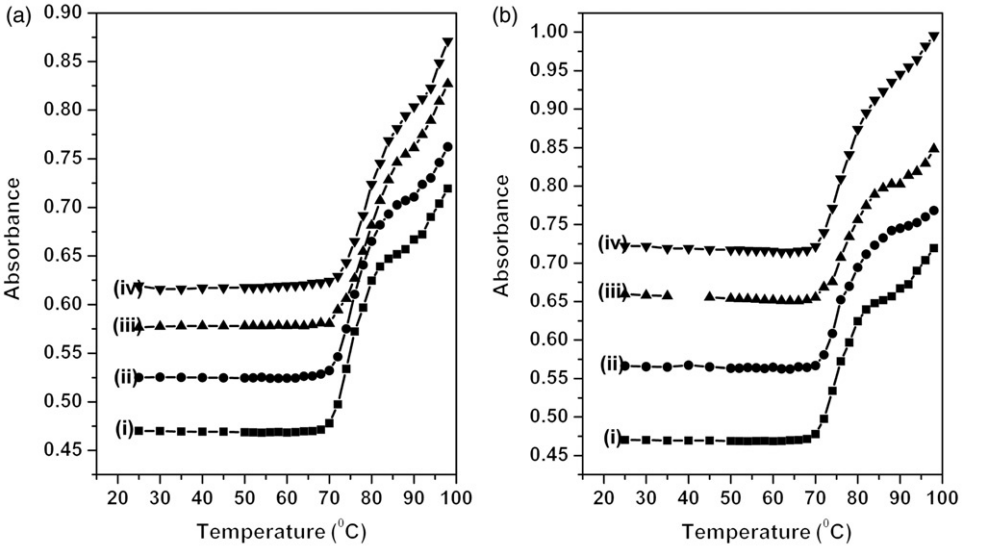


Figure 7. Melting curves of CT-DNA (60 μmol $L^{-1}$) in the absence (i) and presence of 3 μmol $L^{-1}$ (ii); 5 μmol $L^{-1}$ (iii); 7 μmol $L^{-1}$ (iv) of **1**, (a) and **2**, (b).

non-bonded, is a valuable parameter. Generally, intercalation of small molecules results in a considerable stabilization of DNA which corresponds to increase in melting temperature [48]. The melting temperature of DNA was 75°C under our experimental conditions. Under the same set of conditions, addition of **1** and **2** (figure 7) get minor increases to *ca* 77°C ($\Delta T_m$ ~2°C) suggesting DNA binding is primarily electrostatic or groove binding.

Table 2. *In vitro* antimicrobial activity of synthesized complexes and gentamycin sulfate.

| | Diameter of inhibition zone in mm ± SE[a] | | | | | | | | |
|---|---|---|---|---|---|---|---|---|---|
| | *E. coli* | | | *K. pneumoniae* | | | *P. mirabilis* | | |
| Complex | (0.1 mg mL$^{-1}$) | (1 mg mL$^{-1}$) | (2 mg mL$^{-1}$) | (0.1 mg mL$^{-1}$) | (1 mg mL$^{-1}$) | (2 mg mL$^{-1}$) | (0.1 mg mL$^{-1}$) | (1 mg mL$^{-1}$) | (2 mg mL$^{-1}$) |
| **1** | 7.0 ± 0.6a | 10.3 ± 0.9 | 22.3 ± 0.9b | 9.3 ± 0.9 | 10.0 ± 0.6a | 14.0 ± 0.6a | 8.3 ± 0.3 | 11.3 ± 0.3b | 16.7 ± 0.3b |
| **2** | 8.7 ± 0.9ab | 12.3 ± 0.9 | 27.0 ± 0.6c | 10.0 ± 0.6 | 15.3 ± 0.3b | 34.3 ± 0.3b | 8.0 ± 0.6 | 9.0 ± 0.6b | 9.3 ± 0.3a |
| Gentamycin sulfate | | | 50.0 ± 0.3 | | | 42.0 ± 0.3 | | | 46.7 ± 0.7 |

Mean value of the three replicates of three repeated experiments of each test.
Diameter of inhibition zone induced by DMSO in *E. coli*, *K. pneumoniae*, and *P. mirabilis* are 6.0 ± 0.3, 7.0 ± 0.7, and 8.0 ± 0.6.
Data were subjected to one-way analysis of variance followed by Tukey's test. Values are presented as means ± SE.
[a]Represents the diameter of inhibition zone after subtracting the inhibition zone induced by DMSO.
$p < 0.05$ were considered significant.

### 3.6. *Antimicrobial activity*

Ismail [49] reported biological activity studies of copper(II) complexes of an antipyrine Schiff base and discussed the major factors affecting the activities of metal complexes in connection with the structure of the complex, electronic state of the copper, and the copper content in the complex. In bridged dimers, the copper content is higher and the metal center is more exposed structurally as compared to *bis*-ligand complexes. Such exposure facilitates the attachment of substrates to the metal center and thus increases the biological activity. In order to investigate further the relation between biological activities and binuclear copper(II) complexes having different structures, we have chosen **1** and **2** for this study.

The results of antimicrobial activity of **1** and **2** are summarized in table 2. The two complexes show good antibacterial activity against all the tested bacteria. Complex **1** has moderate antibacterial activity against *Escherichia coli* and *Klebsiella pneumonia*e, while **2** shows moderate activity against *Proteus mirabilis*. The chelating activity tends to make the complexes more potent bactericidal agents [50–52]. The chelated complexes deactivate various cellular enzymes, which play a vital role in metabolic pathways of the bacteria. The increased antimicrobial activity of **2** over **1** is probably due to its conjugation effect. Urolithiasis is one of the most common diseases faced by the human society. It is synonymous to calculus formation in the urinary collecting system but most often calculus arises in the kidney. Organisms commonly encountered in urinary tract infection include *E. coli*, *Klebsciella* spp., *Proteus* spp., *Pseudomonas* spp., *Streptococcus* spp., etc. It has been reported that 20% of strains of *E. coli* responsible for urinary tract infection in patients carry transferrable resistance determinants and are resistant to several antimicrobial drugs. *Klebsiella aerogenes* strains are resistant to a wider range of antibiotics than most *E. coli* strains [53]. The present investigation strongly suggests that both the binuclear complexes possess potent antimicrobial activity that could inhibit the growth of pathogenic bacteria. They would provide a potential alternative to antibiotics for controlling some of the microorganisms causing urolithiasis.

## 4. Conclusions

From magnetic moment values and EPR intensity with lowering of temperature, $[Cu(II)(1\text{-phenylamidino-O-methylurea})_2(H_2O)]_2(Cl_2)_2$ forms an antiferromagnetically coupled binuclear complex. However, $[Cu(II)(1\text{-phenylamidino-O-i-butylurea})tmen]_2(Cl_2)_2 \cdot 2H_2O$ exists as a ferromagnetically coupled copper(II) binuclear complex. Absorption titration studies with thermal denaturation studies of the two complexes show that they bind to DNA by electrostatic or groove binding. DNA binding of the complexes is also supported from fluorescence spectroscopic studies. The two complexes inhibit the growth of urolithiatic microorganisms.

## Acknowledgments

One of the authors (S. Pramodini Devi) is grateful to DST, Government of India, for financial support under DST-Women Scientist Scheme-A.

## References


[1] T. Miura, A. Hori-I, H. Mototani, H. Takeuchi. *Biochem.*, **38**, 11560 (1999).
[2] C.J. Burrows, J.G. Muller. *Chem. Rev.*, **98**, 1109 (1998).
[3] J.K. Barton, A. Danishefsky, J. Goldberg. *J. Am. Chem. Soc.*, **106**, 2172 (1984).
[4] R.S. Rajski, R.M. Williams. *Chem. Rev.*, **98**, 2723 (1998).
[5] F. Mancin, P. Scrimin, P. Tecilla, U. Tonellato. *Chem. Commun.*, 2540 (2005).
[6] J.L. Garcia-Gimenez, G. Alzuet, M. Gonzalez-Alvarez, A. Castineiras, M. Liu-Gonzalez, J. Borras. *Inorg. Chem.*, **46**, 7178 (2007).
[7] O.S. Ibopishak, M. Damayenti, N.S. Rajen, R.K.S. Hemakumar, M. Manoj, R.M. Kadam. *Polyhedron*, **24**, 909 (2005).
[8] S.I. Ohkashi, K. Hashimoto. *Chem. Phys. Lett.*, **314**, 210 (1999).
[9] G. Christou, S.P. Perlepes, E. Libby, K. Folting, J.C. Huffman, R.J. Webb, D.N. Hendrickson. *Inorg. Chem.*, **29**, 3657 (1990) and references therein.
[10] (a) U. Suksangpanya, A.J. Blake, P. Hubberstey, C. Wilson. *CrystEngComm*, **6**, 70 (2004) and references therein; (b) M.J. Begley, P. Hubberstey, C.H.M. Moore. *J. Chem. Res. Synop.*, 334 (1991); (c) M.J. Begley, P. Hubberstey, C.H.M. Moore. *J. Chem. Res. Synop.*, 172 (1986); (d) A.J. Black, P. Hubberstey, U. Suksangpanya, C. Wilson. *J. Chem. Soc., Dalton Trans.*, 3873 (2000); (e) U. Suksangpanya, A.J. Blake, P. Hubberstey, D.J. Parker, S.J. Teat, C. Wilson. *Cryst. Eng. Comm.*, **5**, 23 (2003).
[11] J.R.J. Sorenson. In *Handbook on Metal-Ligand Interactions in Biological Fluids: Bioinorganic Medicine*, G. Berthon (Ed.), Vol. 2, p. 1128, Marcel Dekker, New York (1995).
[12] U. Chaveerach, A. Meenongwa, Y. Trongpanich, C. Soikum, P. Chaveerach. *Polyhedron*, **29**, 731 (2010).
[13] S.D. Pramodini, R.K.S. Hemakumar. *Asian J. Chem.*, **22**, 5504 (2010).
[14] L.S. Ajitkumar, O.S. Ibopishak, A.S. Manihar, R.K.S. Hemakumar, R.M. Kadam, M.K. Bhide, A.R. Dhobale, M.D. Sastry. *Spectrochim. Acta (A)*, **60**, 1593 (2004).
[15] S.D. Pramodini, R.K.S. Hemakumar, R.M. Kadam. *Inorg. Chem.*, **45**, 2193 (2006).
[16] S.D. Pramodini, S.D. Mimoda, N.D. Shantibala, R.K.S. Hemakumar, M. Manoj, R.M. Kadam. *Inorg. Chem. Commun.*, **11**, 1441 (2008).
[17] L.S. Jaideva, N.D. Shantibala, S.D. Pramodini, W.D. Bembee, R.K.S. Hemakumar, B. Rajeswari, R.M. Kadam. *Inorg. Chem. Commun.*, **13**, 365 (2010).
[18] F.H.S. Curd, F.L. Rose. *J. Chem. Soc.*, 729 (1946).
[19] R.L. Dutta, A.S. Manihar. *J. Inorg. Nucl. Chem.*, **40**, 417 (1978).
[20] M.E. Reichmann, S.A. Rice, C.A. Thomas, P. Doty. *J. Am. Chem. Soc.*, **76**, 3047 (1954).
[21] J. Marmur. *J. Mol. Biol.*, **3**, 208 (1961).
[22] A. Wolf, G.H.J. Shimer, T. Meehan. *Biochem.*, **26**, 6392 (1987).
[23] M. Lee, A.L. Rhodes, M.D. Wyatt, S. Forrow, J.A. Hartley. *Biochem.*, **32**, 4237 (1993).
[24] C.H. Collins, P.M. Lyne, J.M. Grange. *Microbacterial Methods*, 6th Edn, p. 155, Butterworth & Co. Ltd., London (1989).
[25] J.R. Wasson, C. Trapp. *J. Phys. Chem.*, **73**, 3763 (1969).
[26] A. Das, A. Bagchi, S.R. Saha. *Indian J. Chem. (A)*, **29**, 361 (1990).
[27] M. Jamnicky, P. Segla, M. Koman. *Polyhedron*, **14**, 1837 (1995).
[28] L.S. Ajitkumar, O.S. Ibopishak, A.S. Manihar, R.K.S. Hemakumar, R.M. Kadam, M.K. Bhide, M.D. Sastry. *Transition Met. Chem.*, **26**, 532 (2001).
[29] P.F.B. Barnard. *J. Chem. Soc. (A)*, 2140 (1969).
[30] K. Nakamoto. *Infrared and Raman Spectra of Inorganic and Coordination Compounds*, 4th Edn, pp. 228–229, John Wiley & Sons, New York (1986).
[31] K.N. Krishna, P.S. Vinod. *Transition Met. Chem.*, **21**, 507 (1996).
[32] R. Silverstein, G.C. Bassler. *Spectrometric Identification of Organic Compounds*, Vol. 86, 2nd Edn, Wiley, New York (1967).
[33] G. Ponticelli. *Inorg. Chim Acta*, **5**, 461 (1971).
[34] C.R. Deltcheff, R. Thouvenot, R. Franck. *Spectrochim. Acta (A)*, **32**, 587 (1976).
[35] V. Indira, P.A. Joy, N.A. Alekar, S. Gopinathan, C. Gopinathan. *Indian J. Chem. (A)*, **36**, 687 (1997).
[36] G.H. Jan, B.D.J.M. Preez, V. Brecht. *J. Chem. Soc., Dalton Trans.*, 253 (1989).
[37] E.M. Szablewska, A.S. Waniewska, K. Swiatek, N. Nedelko, M. Golebiewski. *Phys. Status Solidi A*, **196**, 213 (2003).
[38] M. Chikira, H. Kon. *J. Chem. Soc., Dalton Trans.*, 245 (1979).
[39] N.D. Chasteen, R.L. Belford. *J. Inorg. Chem.*, **9**, 169 (1970).
[40] A. Aboukais, A. Bennani, C.F. Aissi, G. Wrobel, M. Guelton, J.C. Vedrine. *J. Chem. Soc., Faraday Trans.*, **88**, 615 (1992).
[41] S.S. Eaton, K.M. More, B.M. Sawant, G.R. Eaton. *J. Am. Chem. Soc.*, **105**, 6560 (1983).
[42] C.J. Burrows, J.G. Muller. *Chem. Rev.*, **98**, 1109 (1998).
[43] S.A. Tysoe, R.J. Morgan, A.D. Baker, T.C. Strekas. *J. Phys. Chem.*, **97**, 1707 (1993).

[44] T.M. Kelly, A.B. Tossi, D.J. McConnell, C. Ohuigin. *Nucleic Acids Res*., **17**, 6017 (1985).
[45] Q.S. Li, P. Yang, H.F. Wang, M.L. Guo. *J. Inorg. Biochem*., **64**, 181 (1996).
[46] B.C. Baguley, M.L. Bret. *Biochemistry*, **23**, 937 (1984).
[47] B. Selvakumar, V. Rajenderan, P.U. Maheswari, H.S. Evans, M. Palaniandavar. *J. Inorg. Biochem*., **100**, 316 (2006).
[48] C.V. Kumar, E.H. Asuncion. *J. Am. Chem. Soc*., **115**, 8547 (1993).
[49] K.Z. Ismail. *Transition Met. Chem*., **25**, 522 (2000).
[50] S. Belaid, A. Landreau, S. Djebbar, O. Benali-Baitich, G. Bouet, J.P. Bouchara. *J. Inorg. Biochem*., **102**, 63 (2008).
[51] M. Tumer, H. Koksal, M.K. Sener, S. Serin. *Transition Met. Chem*., **24**, 414 (1999).
[52] N. Raman, A. Sakthivel, R. Jeyamururgan. *J. Coord. Chem*., **63**, 1080 (2010).
[53] Topley and Wilson's *Principles of Bacteriology, Virology and Immunity*, Vol. 1, Chap. 26, pp. 859–900 (1975).